# Large Eddy Simulation of transcritical flows

**Thomas Schmitt**[1], **Bénédicte Cuenot**[1]

[1]Centre d'Étude, de Recherche et de Formation Avancée
en Calcul Scientifique (CERFACS),
31057 Toulouse, France

## 1 Introduction

In a liquid propellant rocket engine, the high pressure chamber allows a high specific impulse, increasing the overall efficiency of the engine. For example, in the Vulcain engine, that powers the Ariane 5 launch vehicle, the chamber reaches 115 *bars*, which is above the critical pressure of the injected propellants. Oxygen is injected at a cold, subcritical temperature in a supercritical environment, and thus will experience a transcritical injection.

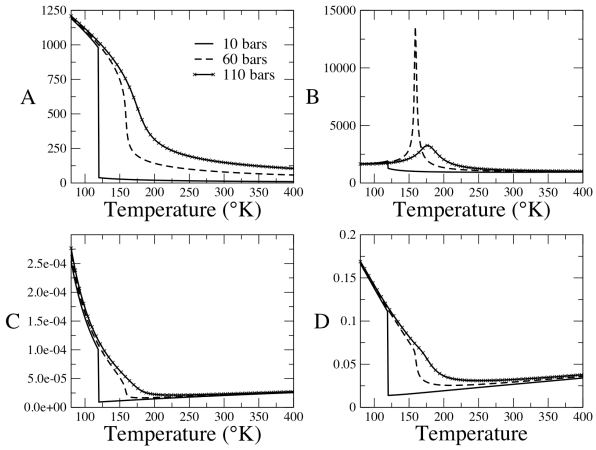


Figure 1: Oxygen properties for severals pressures (NIST database). A : density ($kg.m^{-3}$), B : Cp ($J.kg^{-1}$), C : Dynamic viscosity ($kg.(m.s)^{-1}$), D : thermal conductivity ($W.(m.K)^{-1}$).

Figure 1 shows the density, heat capacity, viscosity and thermal conductivity of oxygen for several pressures. Above the critical pressure (50.4 *bars*), surface tension goes to zero. As a consequence, dense and light fluids may coexist without any interface between the two, leading to high density gradients. In the near critical temperature zone (154,6 K), fluids properties become very sensitive to changes in temperature. In particular, the heat capacity at constant pressure becomes extremely large. In contrast to low pressure liquid jets, the injected dense fluid does no longer undergo the classical atomization sequence : diminished intermolecular forces promote diffusion dominated processes that are affected by the presence of huge gradients. The strong properties variation also affects the jet dynamics. In the case of a coaxial $LO_X$ / $GH_2$ reactive jet, a diffusion dominated mode of combustion occurs and the flame is anchored by recirculation zones just downstream of the injector lips.

Several experiments focused on supercritical fluid injection and mixing have been conducted (Oschwald et al. [1]). They give access to quantitative results for the non reactive case of single and coaxial high pressure jet. Recent modeling and simulation advances can be found in the papers of Yang and Zong [2] and Oefelein [3], however, the current state of the art is mainly concerned with Direct Numerical Simulation (DNS) and fine meshes Large Eddy Simulation (LES).

The present study uses the LES code AVBP, developed at Cerfacs for combustion applications. Initially developed for low pressure cases and based on perfect gas thermodynamics and transport models,

**Correspondence to : thomas.schmitt@cerfacs.fr** 

AVBP has been adapted to high pressure flows.

The high pressure model, its numerical implementation and its validation is presented in detail below. Then the simulation of a real configuration is shown and compared to experimental data.

# 2 Modelling

To correctly evaluate the thermodynamic properties at high pressure, a real gas equation of state is needed. In this study, the Peng-Robinson equation of state [4] (eq. 1), with the classical Van Der Waals mixing rules [5], has been chosen for its accurate behaviour in the range of pressure and temperature of interest. The Peng-Robinson equation reads:

$$P = \frac{RT}{v - b_m} - \frac{a_m(T)}{v^2 + 2vb_m - b_m^2} \tag{1}$$

where $P$ is the pressure, $T$ the temperature, $v = \frac{V}{n}$ the molar volume ($n$ is the number of mole) and $R$ the gas constant. $a_m(T)$ and $b_m$ are the Peng-Robinson coefficients [4] for the mixture considered.

The density effects that occur near and above the critical temperature are taken into account using departure functions, directly obtained from the equation of state. An example of such a departure function is given in Eq. 2 for the internal energy $e$. In this expression, $e_0(T)$ is the reference energy at low density, which depends only on temperature and composition. The term on the right hand side of Eq. 2 is obtained from fundamental thermodynamic relations.

$$e - e^0(T) = -\int_v^{v_0} \left\{ T\left(\frac{\partial P}{\partial T}\right)_{v,X_k} - P \right\}_{T,X_k} dv \tag{2}$$

Enthalpy and heat capacities are calculated using the same procedure.

Unlike in the perfect gas case, the temperature can not be directly obtained from internal energy and composition, because of its additional pressure dependence. Therefore an inversion method (like an iterative method for example) is needed to calculate the temperature from internal energy, density and mass fractions.

Viscosity and thermal conductivity of mixtures are calculated using the method described by Chung et al. [6]. In this study, the Soret and Dufour effects are neglected, since they have been shown to be very small compared to ordinary diffusion in the case of LOX-H2 combustion [3]. More generally they are likely to be hidden by turbulent mixing in most cases.

# 3 Numerical implementation

Modifying the thermodynamics properties of the code has several effects on the numerical algorithms.

Most numerical schemes used in complex geometries simulations require the calculation of a non-viscous jacobian matrix. Since the relation between the energy, density, pressure and mass fractions has been changed, this matrix must be updated. For example, in the case of the Lax-Wendroff scheme, the modification of the matrix is reduced to the implementation of the modified differential of the pressure.

The other main numerical modification concerns the boundary conditions that are classically based on the method of characteristics for compressible flows [7]. It can be shown that the characteristic variables for a real gas have the same expressions as for a perfect gas. However, the sound speed has a modified expression given in eq. 3, where $\overline{W}$ is the mean molar mass, $\rho$ is the density $\kappa_s$ is the isentropic compressibility, $\beta$ is the isothermal compressibility and $\gamma = \frac{C_p}{C_v}$.

$$c^2 = \frac{1}{\rho \kappa_s} = \frac{\gamma}{\rho}\frac{1}{\beta} \tag{3}$$

# 4 Validation of the real gas thermodynamic model

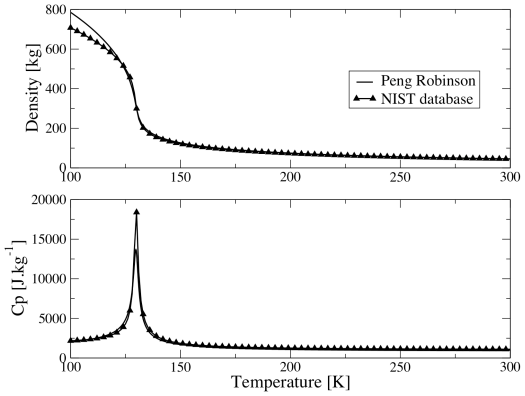


Figure 2: Density (top) and heat capacity at constant pressure (bottom) for $N_2$ at 40 bars in terms of temperature and compared to the NIST database.

Series of zero-dimensional test cases have been performed to check the correct behaviour of the model.

Examples of thermodynamic results for $N_2$ are given on figure 2, where the density and heat capacity at constant pressure are plotted in terms of temperature and compared with the NIST database (webbook.nist.gov/chemistry/fluid/). Results are in good agreement with the reference in most of the considered temperature range. Only in very dense fluids, density is over evaluated by maximum 10%. This is a classical behaviour of the Peng-Robinson equation of state [4], that can be compensated using a volume correction [8]. The capacity of the numerical scheme to handle high density gradients has been checked on convection cases, without diffusion, of a two species ($H_2/O_2$) entropic wave in a one dimensional periodic domain.

# 5 Application to a turbulent jet

The 2D simulation of a single non-reacting mono-species jet is presented here. The numerical domain and configuration, which corresponds to the Oschwald experiment in $N_2$ single jet [1] with the injection speed increased to 20 $m.s^{-1}$, is described in figure 3. The injector diameter is 1.9 mm. The chamber pressure is initialy at 40 bars and 298 K. $N_2$ is injected at 140 K. The critical pressure and temperature of the $N_2$ are 34.958 bars and 126.92 K, then the injected $N_2$ is at supercritical temperature. Under these conditions, the jet density approaches 160 $kg.m^{-3}$ while the reservoir density is 45 $kg.m^{-3}$.

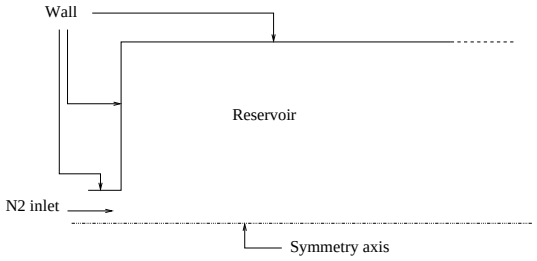


| Element type | triangles |
|---|---|
| Number of nodes | 4904 |
| Scheme | TTGC (order 3 in space) |
| Reynolds number | $\approx 4 \times 10^5$ |

Figure 3: Sketch of the computing domain and table of the main numerical characteristics.

Results are shown for the stable regime reached after several convective times. Figure 4 (left) represents the compressibility factor $Z = \frac{pv}{RT}$ (one in a perfect gas). Real gas effects are present since the compressibility factor range is between 0.6 and 1. The speed magnitude (fig. 4, right) shows the jet destabilization and the first stages of transition to turbulence. Boundary conditions behave correctly, as both the inlet and outlet respect target conditions without introducing spurious numerical waves.

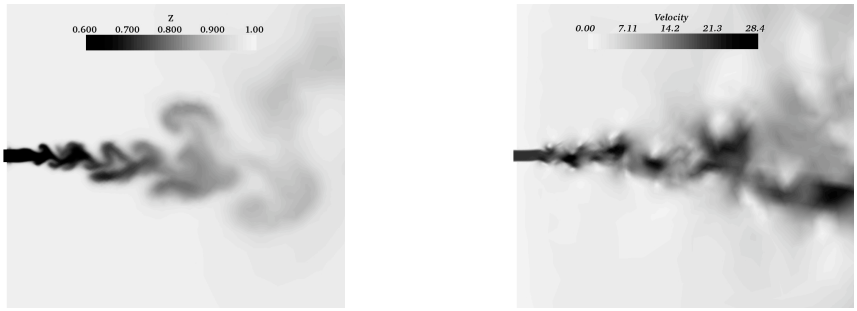


Figure 4: Compressibility factor field (left) and velocity magnitude ($m.s^{-1}$) (right) fields.

# 6 Conclusion

A real gas thermodynamic model has been implemented in AVBP, developed at CERFACS, in order to perform Large Eddy Simulation of reacting flows in liquid rocket engines. A series of test cases has shown the good behaviour of the model compared to reference thermodynamic data. The simulation of a turbulent jet under supercritical conditions has confirmed that the real gas model implemented in AVBP is able to simulate supercritical effects in turbulent unsteady flows with density gradients, and that the implemented numerical schemes are able to handle such flows. Currently research is focused on numerical schemes in order to improve the accuracy of pressure calculation in stronger gradient zone than the ones currently studied. The next step is the validation of the model by confrontating it to experimental results (Oschwald et al. [1]).

**Acknowledgements**-The support of CNES and Snecma (SAFRAN Group) is greatly acknowledged.

# References

[1] M. Oschwald, J. J. Smith, R. Branam, J. Hussong, A. Shik, B. Chehroudi, D. Talley (2006). Injection of fluids into supercritical environments. Combustion Science and Technology, 178: 49-100

[2] Nan Zong, Vigor Yang (2006). Cryogenic fluid jets and mixing layers in transcritical and supercritical environment. Combustion Science and Technology, 178: 193

[3] Joseph C. Oefelein (2006). Mixing and combustion of cryogenic oxygen-hydrogen. Combustion Science and Technology, 178: 229

[4] Ding-Yu Peng, Donald B. Robinson (1976). A new two-Constant Equation of State. Industrial & Engineering Chemistry Fundamentals, 15: 59

[5] B. E. Poling, J.M. Prausnitz, J. P. O'Connel (2001). The properties of gases and liquids, Fifth edition. McGraw-Hill

[6] T.H. Chung, M. Ajlan, L.L. Lee, K.E. Starling (1988). Generalized multiparameter corresponding state correlation for polyatomic, polar fluid transport properties. Industrial and Chemical Engineering Research, 27: 671

[7] T. Poinsot, S. Lele (1992). Boundary conditions for direct simulations of compressible viscous flows. Journal of Computational Physics, 101: 104-129

[8] Paul M. Mathias, Tarik Naheiri and Edwin M. Oh (1989). A density correction for the Peng-Robinson equation of state. Fluid Phase Equilibria, 47: 77-87